

## Evaluation of the Antiproliferative Activity of Diterpene Isonitriles from the Sponge *Pseudoaxinella flava* in Apoptosis-Sensitive and Apoptosis-Resistant Cancer Cell Lines

Delphine Lamoral-Theys,<sup>†</sup> Ernesto Fattorusso,<sup>†</sup> Alfonso Mangoni,<sup>†</sup> Cristina Perinu,<sup>†</sup> Robert Kiss,<sup>§</sup> and Valeria Costantino<sup>\*,†</sup>

<sup>†</sup>The NeaNAT Group, Dipartimento di Chimica delle Sostanze Naturali, Università degli Studi di Napoli Federico II, Via D. Montesano 49, 80131 Napoli, Italy

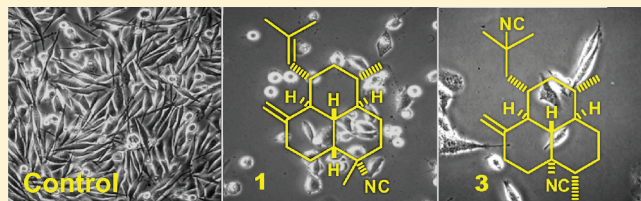
<sup>‡</sup>Laboratoire de Chimie Analytique, Toxicologie et de Chimie Physique Appliquée, Faculté de Pharmacie, Université Libre de Bruxelles, Campus de la Plaine, Boulevard du Triomphe, 1050 Brussels, Belgium

<sup>§</sup>Laboratoire de Toxicologie, Faculté de Pharmacie, Université Libre de Bruxelles, Campus de la Plaine, Boulevard du Triomphe, 1050 Brussels, Belgium

**S** Supporting Information

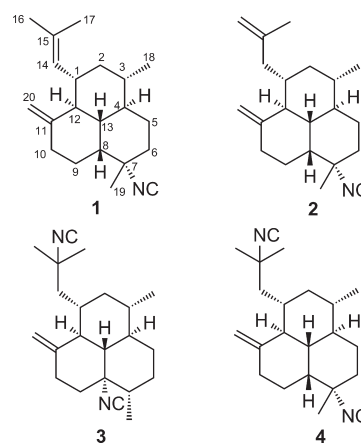
**ABSTRACT:** One new (**1**) and three known (**2–4**) isonitrile diterpenes, isolated from the Caribbean sponge *Pseudoaxinella flava*, were assayed in human cancer cell lines in vitro using an MTT colorimetric assay and quantitative videomicroscopy. Compounds **1–4** displayed activity for human PC3 prostate apoptosis-sensitive cancer cell lines. Compounds **3** and **4** demonstrated similar growth inhibitory effects for three apoptosis-sensitive and three apoptosis-resistant cancer cell lines.

Quantitative videomicroscopy analysis revealed that compounds **1** and **2** exerted their activity through cytotoxic effects, and compounds **3** and **4** through cytostatic effects. These results identify marine diterpene isonitriles as potential lead compounds for anticancer drug discovery.



Terpenoids that contain isocyano and isothiocyano groups are secondary metabolites often found in marine invertebrates, such as sponges.<sup>1</sup> During the last fifteen years, members of this unusually functionalized class of marine natural products have attracted wide interest in the scientific community because of their bioactivity. In fact, one of the most potent marine antimalarial compounds is a diterpene isonitrile that was originally isolated from a tropical sponge and is characterized by an amphilectane skeleton.<sup>2,3</sup> In the framework of our research program, which identifies novel lead compounds that can be used as models in anticancer assays, the chemistry of the Caribbean sponge *Pseudoaxinella flava* was studied. This study led to the isolation of one new diterpene isonitrile compound (**1**) and three known analogues (**2–4**), all of which are closely related to each other but differ in the number and position of the isonitrile functional groups and double bonds.

Diterpenes **1–4** were tested at different concentrations on various human cancer cell lines using the colorimetric MTT assay to evaluate the IC<sub>50</sub> growth inhibitory concentration (i.e., the concentration that decreases by 50% the global growth of a given cell population cultured for three days with the compound of interest) in vitro.<sup>4–7</sup> Quantitative videomicroscopy (i.e., computer-assisted phase-contrast microscopy) was then used to determine whether the antiproliferative effects proceeded through cytotoxic or cytostatic pathways. We have already successfully performed



such characterization for other types of compounds, including fungal secondary metabolites,<sup>4</sup> cardiotonic steroids,<sup>5</sup> and Amaryllidaceae alkaloids.<sup>6,7</sup>

Samples of the sponge *Pseudoaxinella flava*, collected by scuba along the coast of the Grand Bahamas (Sweeting Cay) during the 2007 Pawlik expedition, were cut immediately into small pieces

Received: June 15, 2011

Published: October 10, 2011

Table 1. NMR Spectroscopic Data (700 MHz, CDCl<sub>3</sub>) for Compound 1

position		$\delta_{\text{H}}$ (J in Hz)	$\delta_{\text{C}}$ , type	COSY	HMBC <sup>d</sup>
1		2.35, dddd (11.5, 10.4, 9.0, 4.0)	38.2, CH	2 $\alpha$ , 2 $\beta$ , 12, 14	
2	$\alpha$	0.93, ddd (13.5, 11.5, 11.5)	42.7, CH <sub>2</sub>	1, 2 $\beta$ , 3	1, 12, 14, 18
	$\beta$	1.64, ddd (13.5, 4.0, 4.0)		1, 2 $\alpha$ , 3	12
3		1.21 <sup>a</sup>	39.8, CH	2 $\alpha$ , 2 $\beta$ , 4, <sup>b</sup> H <sub>3</sub> -18	
4		1.28, m	40.5, CH	3, <sup>b</sup> 5 $\alpha$ , 5 $\beta$ , 13 <sup>b</sup>	
5	$\alpha$	1.97, dddd (14.2, 6.8, 6.8, 6.8)	24.7, CH <sub>2</sub>	4, 5 $\beta$ , 6 $\alpha$ , 6 $\beta$	4, 6, 7, 13
	$\beta$	1.08, dddd (14.2, 10.2, 6.6, 6.6)		4, 5 $\alpha$ , 6 $\alpha$ , 6 $\beta$	6, 7
6	$\alpha$	1.81, ddd (13.4, 6.6, 6.6)	34.0, CH <sub>2</sub>	5 $\alpha$ , 5 $\beta$ , 6 $\beta$ , 19 <sup>c</sup>	4, 5, 7, 8, 19
	$\beta$	1.60, m		5 $\alpha$ , 5 $\beta$ , 6 $\alpha$	4, 5, 7, 8
7			59.8, C		
8		1.50, m	42.4, CH	9 $\alpha$ / $\beta$ , 13	9, 10, 13
9	$\alpha,\beta$	1.77, m	21.3, CH <sub>2</sub>	8	13
10	$\alpha$	2.46, brd (15.4)	33.0, CH <sub>2</sub>	9 $\alpha$ / $\beta$ , 10 $\beta$ , 20 $\text{proE}$ , <sup>c</sup> 20 $\text{proZ}$ <sup>c</sup>	
	$\beta$	2.23, ddd (15.4, 9.5, 9.5)		9 $\alpha$ / $\beta$ , 10 $\alpha$ , 20 $\text{proE}$ , <sup>c</sup> 20 $\text{proZ}$ <sup>c</sup>	9, 11, 12, 20
11			148.2, C		
12		1.74, t (10.4)	49.5, CH	1, 13, 20 $\text{proE}$ , <sup>c</sup> 20 $\text{proZ}$ <sup>c</sup>	2, 12, 20
13		1.22 <sup>a</sup>	44.6, CH	4, <sup>b</sup> 8, 12	
14		4.78, brd (9.0)	129.6, CH	1, 16, <sup>c</sup> 17 <sup>c</sup>	1, 16, 17
15			129.2, C		
16		1.65, brs	25.7, CH <sub>3</sub>	14 <sup>c</sup>	14, 15, 17
17		1.63, brs	17.9, CH <sub>3</sub>	14 <sup>c</sup>	14, 15, 17
18		0.89, d (6.3)	19.3, CH <sub>3</sub>	3	2, 3, 4
19		1.41, brs	28.9, CH <sub>3</sub>	6 $\alpha$ <sup>c</sup>	6, 7, 8
20	pro-E	4.76, brs	107.4, CH <sub>2</sub>	10 $\alpha$ , <sup>c</sup> 10 $\beta$ , <sup>c</sup> 12, <sup>c</sup> 20 $\text{proZ}$	10, 11, 12
	pro-Z	4.48, brs		10 $\alpha$ , <sup>c</sup> 10 $\beta$ , <sup>c</sup> 12, <sup>c</sup> 20 $\text{proE}$	10, 11, 12
21			154.5, C		

<sup>a</sup> Overlapping signals. <sup>b</sup> Overlapping cross-peaks. <sup>c</sup> Long-range coupling (allylic or *W*-coupling). <sup>d</sup> HMBC correlations are from proton(s) stated to indicated carbon.

and frozen. The samples were then shipped to the laboratory and extracted sequentially with MeOH and CHCl<sub>3</sub>. The MeOH extract was dried and partitioned between water and BuOH, and the combined BuOH and CHCl<sub>3</sub> extracts were subjected to reversed-phase column chromatography. The fraction eluted with MeOH–H<sub>2</sub>O (9:1) contained diterpene isonitrile compounds, which were first purified on a silica gel column and then by HPLC using *n*-hexane–EtOAc (95:5) as the eluent. Compounds **3** and **4** were obtained in high purity, whereas compounds **1** and **2** were eluted as a mixture. This mixture was subjected to an additional HPLC separation (silica gel, 0.05% *i*-PrOH in *n*-hexane) to yield the pure compounds **1** and **2**. The structures of the known compounds **2**–**4** were confirmed by comparing their MS, <sup>1</sup>H NMR, <sup>13</sup>C NMR, and optical rotation data with those reported in the literature<sup>8,9</sup> (spectroscopic data are reported in ref 8, whereas subsequently revised structures are reported in ref 9).

A high-resolution ESIMS measurement of compound **1** showed an [M + Na]<sup>+</sup> pseudomolecular ion peak at *m/z* 320.2351 (C<sub>21</sub>H<sub>31</sub>NNa), corresponding to the molecular formula C<sub>21</sub>H<sub>31</sub>N. Compound **1** is therefore isomeric with compound **2**. The fragment peak at *m/z* 293.2234 (C<sub>20</sub>H<sub>30</sub>Na) present in MS/MS was due to the loss of HCN. These peaks, together with the signal at  $\delta$  154.5 in the <sup>13</sup>C NMR spectrum, indicated the presence of an isonitrile group in compound **1**. Analysis of the COSY, HSQC, and HMBC two-dimensional NMR experiments of compound **1** showed the planar structure of the tricyclic skeleton of **1** to be identical to that of compound **2** and allowed assignment of

all the relevant <sup>1</sup>H and <sup>13</sup>C NMR signals (Table 1). However, the signals of the 2-methylallyl side chain (C-14/C-17) of compound **2** were not present in the <sup>13</sup>C NMR spectrum of compound **1**. Instead, two methyl singlets at  $\delta$  1.63 (H<sub>3</sub>-17) and 1.65 (H<sub>3</sub>-16) were observed in the proton spectrum, and both were allylically coupled with the olefinic proton at  $\delta$  4.78 (H-14), as shown by the COSY spectrum. The latter proton was in turn coupled with H-1 ( $\delta$  2.35), thus leading to the identification of an isobutenyl group at C-1. The presence of an isobutenyl group was confirmed from the <sup>13</sup>C NMR spectrum, which exhibited olefinic CH ( $\delta$  129.6, C-14) and C ( $\delta$  129.2, C-15) carbon atoms in addition to the signals for the exocyclic double bond at C-11.

Analysis of the ROESY spectrum was not useful to define the relative configuration of the tricyclic skeleton of compound **1**, because it showed proximity relationships that were inconsistent with a single structure. This suggests the possibility of conformational equilibria, which are indeed possible for the *cis*-decalin partial structure (C-4 through C-13 carbon atoms). This difficulty is confirmed by the fact that the first reported configuration of compound **2**, based on NOE experiments, was incorrect,<sup>8</sup> and only X-ray diffraction analysis allowed the correct configuration to be determined.<sup>9</sup> However, it can be safely assumed that the configuration of the tricyclic skeleton of compound **1** is the same as in compound **2**, because the <sup>13</sup>C NMR resonances of all carbons of the tricyclic system (except for C-1, which is affected by the different side chain) matched within 1 ppm the corresponding resonances of compound **2**.

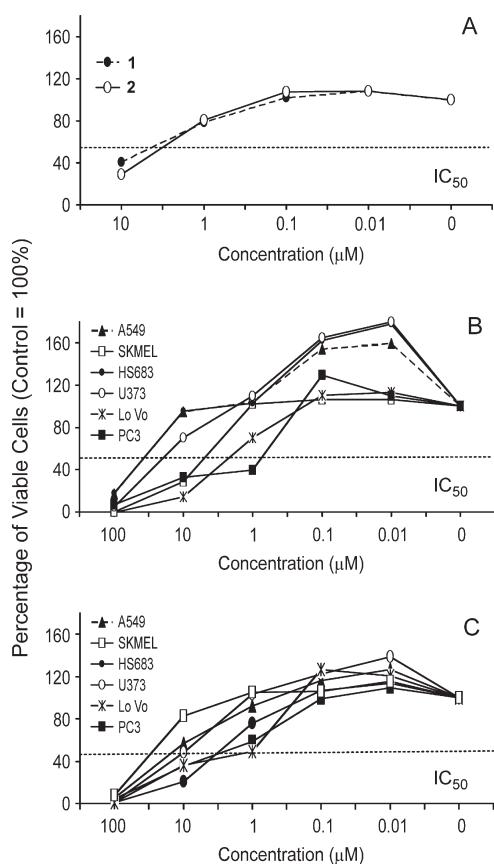


**Figure 1.** MTT colorimetric assay determination of  $IC_{50}$  growth inhibitory concentrations. Compounds **1** and **2** were assayed against the human PC3 prostate cancer cell line (A), while compounds **3** (B) and **4** (C) were assayed against six human cancer cell lines. The SEM values are not reported in this figure for the sake of clarity because they approximately correspond to the sizes of the symbols used.

Only small amounts of compounds **1** and **2** were obtained, so the antiproliferative activities of these compounds were investigated on one cancer cell line, i.e., the human apoptosis-sensitive PC3 prostate cancer cell line,<sup>10</sup> using a MTT colorimetric assay and quantitative videomicroscopy. Compounds **3** and **4** were assayed in parallel with compounds **1** and **2** in this PC3 prostate cancer model and also using five additional human cancer cell lines.

The results obtained as discussed below, while preliminary, must be evaluated with respect to the most recent therapeutic agents developed against cancers, which are unfortunately associated with dismal prognoses. Indeed, before a cancer has metastasized, surgery remains the best treatment for cancer patients because total tumor removal can be curative. In contrast, if the cancer has already metastasized by the time of diagnosis, adjuvant therapies with surgery are essential for combating the disease. These adjuvant therapies include radiotherapy and chemotherapy. More than 80% of the cancer chemotherapeutic drugs used today to treat cancers are proapoptotic agents, although numerous cancer types are naturally resistant to apoptosis, such as gliomas,<sup>17</sup> melanomas,<sup>18</sup> pancreatic cancers,<sup>19</sup> non-small-cell lung cancers,<sup>20</sup> esophageal cancers,<sup>21</sup> and, above all, metastatic cancers.<sup>22,23</sup> It is therefore highly important to identify novel therapeutics that can eliminate apoptotic-resistant cancer cells.

Compounds **1–4** displayed similar growth inhibitory activities for the human PC3 prostate cancer cell line, with  $IC_{50}$

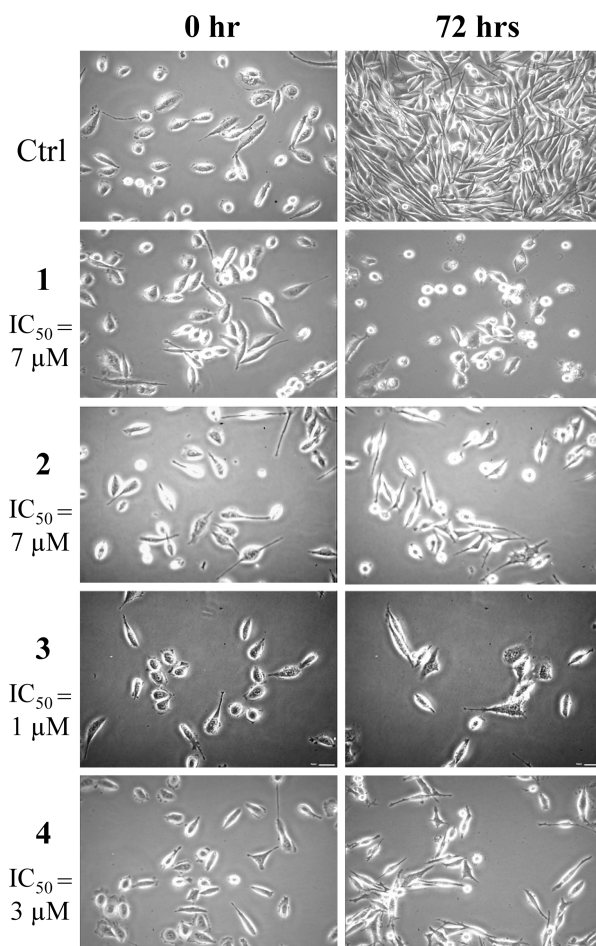


**Figure 2.** Quantitative videomicroscopy analysis of compounds **1–4** at their  $IC_{50}$  concentrations (obtained by means of the MTT colorimetric assay) for the human PC3 prostate cancer cell line. The morphological analyses were carried out at a  $G \times 100$  magnification.

growth inhibitory values of  $7 \pm 1 \mu M$  for **1** and **2** (Figure 1A),  $1 \pm 1 \mu M$  for **3** (Figure 1B), and  $3 \pm 1 \mu M$  for **4** (Figure 1C). The  $IC_{50}$  growth inhibitory concentrations ( $\mu M$ ) for compounds **3** and **4** were  $25 \pm 1$  and  $10 \pm 1$  for U373 glioblastoma,  $50 \pm 2$  and  $4 \pm 1$  for Hs683 oligodendrogloma,  $42 \pm 1$  and  $16 \pm 2$  in A549 NSCLC,  $3 \pm 1$  for both compounds for LoVo colon cancer, and  $6 \pm 1$  and  $32 \pm 1$  for SKMEL-28 melanoma cells, respectively.

While displaying similar  $IC_{50}$  growth inhibitory values for human PC-3 prostate cancer cells, compounds **1–4** do not seem to exert their respective activity through the same mechanism. Indeed, low-magnification morphological analysis suggested that compounds **1** and **2** are active through direct cytotoxic effects, whereas compound **3** and **4** exhibit cytostatic effects, both of which lead to cell death (Figure 2).

Cells that died appeared rounded and refringent under quantitative videomicroscopy analysis. The proportion of this cell type in PC3 prostate cancer cells was higher following treatment with compounds **1** and **2** at their  $IC_{50}$  growth inhibitory concentrations for 72 h than with compounds **3** and **4**. High-magnification morphological analysis confirmed these features (Figure 3). Indeed, compound **1** induced marked vacuolization processes, which in turn, led to cell death (Figure 3). These marked compound **1**-induced vacuolization processes could be due to either

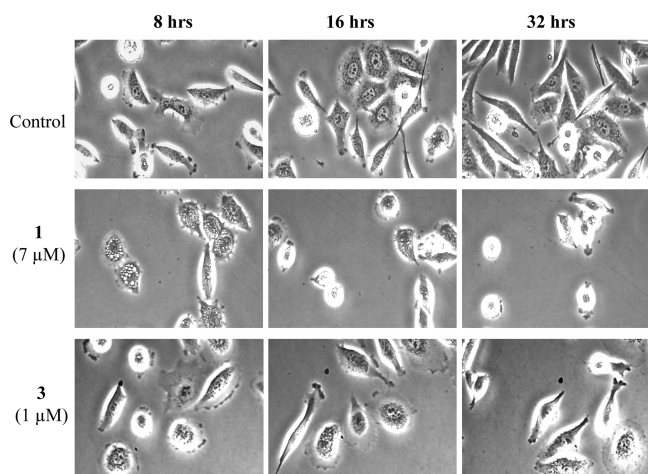


**Figure 3.** Quantitative videomicroscopy analysis of compounds **1** and **3** for the human PC3 prostate cancer cell line. The  $IC_{50}$  values were calculated using the MTT colorimetric assay, and the morphological analyses were carried out at a  $\times 500$  magnification.

lysosomal membrane permeabilization<sup>11</sup> and/or sustained autophagy<sup>12</sup> cell death. In contrast, compound **3** seemed to exert its inhibitory activity through cytostatic effects, i.e., the inhibition of cell proliferation rather than the induction of cell death (Figure 3).

Altogether, these data suggest that when compounds **1** and **2** exert their inhibitory effects through cytotoxic-related mechanisms, cell death processes could occur independently of apoptosis induction based on the absence of pathognomonic morphological features as revealed by the quantitative videomicroscopy approach.

In order to validate this hypothesis at the experimental level, compounds **3** and **4** (for which sufficient amounts were available) were assayed using apoptosis-sensitive cancer cell lines and cancer cell lines resistant to pro-apoptotic stimuli. Three human apoptosis-sensitive cancer cell lines were used, namely, PC3 prostate cancer,<sup>10</sup> Hs683 oligodendroglioma,<sup>13</sup> and LoVo colon cancer.<sup>14</sup> In the same manner, three human cancer cell lines were used that display certain levels of resistance to proapoptotic stimuli: U373 glioblastoma, which is resistant to apoptosis<sup>15</sup> but sensitive to autophagy-related cell death;<sup>12</sup> A549 NSCLC, which is resistant to apoptosis<sup>11</sup> and to autophagy-related cell death,<sup>11</sup> but is sensitive to lysosomal membrane permeabilization-related cell death;<sup>11</sup> and SKMEL-28 melanoma.<sup>16</sup> The data illustrated in Figure 1B (compound **3**) and 1C (compound **4**) indicate that compounds **3** and **4** displayed similar in vitro effects for the three apoptosis-sensitive cancer cell lines (PC3, Hs683, and LoVo) when compared to the three cancer cell lines with various levels of resistance to pro-apoptotic stimuli (U373, A549, SKMEL-28).

Therefore, the preliminary data reported in the current study suggest that the diterpene isonitriles **1–4** represent interesting chemical scaffolds that could be pharmacologically optimized to combat cancer cells that are resistant to proapoptotic stimuli.

## EXPERIMENTAL SECTION

**General Experimental Procedures.** Optical rotations were measured at 589 nm on a JASCO P-2000 polarimeter using a 10 cm microcell. NMR spectra were determined on Varian UnityInova

spectrometers at 500 and 700 MHz; chemical shifts are referenced to the residual solvent signal ( $CDCl_3$ ;  $\delta_H = 7.26$ ,  $\delta_C = 77.0$ ). For an accurate measurement of the coupling constants, the one-dimensional  $^1H$  NMR spectra were transformed at 64K points (digital resolution: 0.09 Hz). Homonuclear  $^1H$  connectivities were determined by a COSY experiment. Through-space  $^1H$  connectivities were calculated using a ROESY experiment with a mixing time of 450 ms. The single-quantum heteronuclear correlation (HSQC) and multiple-bond heteronuclear correlation (HMBC) spectra were adjusted, respectively, for an average  $^1J_{CH}$  of 142 Hz and a  $^{2,3}J_{CH}$  of 8.3 Hz. HRESIMS and ESIMS/MS were performed on a Thermo LTQ Orbitrap XL mass spectrometer. The spectra were recorded by infusion into the ESI source using MeOH as the solvent. HPLC was performed on a Varian Prostar 210 apparatus equipped with a Varian 350 refractive index detector.

**Animal Material.** Specimens of *Pseudoaxinella flava* were collected in June 2007 along the coast of Grand Bahamas (Sweeting Cay, 26°36.369' N, 77°41.713' W) during the 2007 Pawlik expedition and identified by Prof. S. Zea (University of Colombia) aboard the vessel. They were frozen immediately after collection and kept frozen until extraction.

**Extraction and Isolation.** The sponge (220 g of dry weight after extraction) was homogenized and extracted with methanol ( $3 \times 1$  L) and then with chloroform ( $3 \times 1$  L); the combined extracts were partitioned between  $H_2O$  and *n*-BuOH. The organic layer was concentrated in vacuo and afforded 16.3 g of a dark green oil, which was chromatographed on a column packed with RP-18 silica gel. A fraction (825 mg) eluted with  $CH_3OH-H_2O$  (9:1) was further chromatographed on a silica gel column, giving a fraction composed mainly of isonitrile terpenes [250 mg, eluent *n*-hexane–EtOAc (9:1)]. This fraction was subjected to HPLC separation on a silica gel column [eluent: *n*-hexane–EtOAc (95:5)], giving pure compounds **3** (145 mg, 0.9% w/w of crude extract) and **4** (38 mg, 0.2% w/w) and a mixture (21 mg) of compounds **1** and **2**. The mixture was subjected to a further HPLC separation (silica gel column, 0.05% *i*-PrOH in *n*-hexane), giving pure **1** (10.3 mg, 0.06% w/w) and **2** (2.9 mg, 0.02% w/w).

Compound **1**: colorless oil;  $[\alpha]_D^{25} +103$  ( $c$  0.11,  $CHCl_3$ );  $^1H$  and  $^{13}C$  NMR data, see Table 1. HRESIMS (positive ion mode, MeOH)  $m/z$  320.2351  $[M + Na]^+$  (calcd for  $C_{21}H_{31}NNa$ , 320.2349).

**Evaluation of Antiproliferative Activities in Cancer Cell Lines.** The  $IC_{50}$  growth inhibitory values were determined for the compounds under study using the MTT colorimetric assay, as detailed in previous studies.<sup>4–7</sup> The experiments were carried out using a Biorad model 680XR (Biorad, Nazareth, Belgium) at a 570 nm wavelength (with a reference of 630 nm). Each experimental condition was carried out in sextuplicate. The origin of the cell lines used in the current study and the culture media are also fully detailed in prior literature.<sup>4–7,15</sup>

Quantitative videomicroscopy analyses were performed as detailed elsewhere.<sup>4–7</sup>

## ASSOCIATED CONTENT

**Supporting Information.** Spectra of compound **1**; this information is available free of charge via the Internet at <http://pubs.acs.org>.

## AUTHOR INFORMATION

### Corresponding Author

\*Tel: +39 081 678504. Fax: +39 081 678552. E-mail: [valeria.costantino@unina.it](mailto:valeria.costantino@unina.it).

## ACKNOWLEDGMENT

This research work was supported by the FP7 EC Project NatPharma (REGPOT-2008-1, grant agreement no. 229893)

and by the Fonds National de la Recherche Scientifique (FNRS, Belgium). Samples of the sponge *Pseudoaxinella flava* were collected by V.C. during the 2007 Pawlik Bahamas cruise. We wish to thank Prof. J. R. Pawlik (University of North Carolina) for the invitation to the Bahamas cruise and for his help and support in sample collection. We also thank Prof. S. Zea (Departamento de Biología y Centro de Estudios en Ciencias del Mar-CECIMAR, Universidad Nacional de Colombia) for identifying the sponge aboard the vessel. Mass and NMR spectra were recorded at the “Centro di Servizi Interdipartimentale di Analisi Strumentale”, Università di Napoli “Federico II”. The assistance of the staff is gratefully acknowledged.

(23) Wilson, T. R.; Johnston, P. G.; Longley, D. B. *Curr. Cancer Drug Targets* **2009**, *9*, 307–319.

## REFERENCES

- (1) Garson, M. J.; Simpson, J. S. *Nat. Prod. Rep.* **2004**, *21*, 164–179.
- (2) Konig, G. M.; Wright, A. D. *J. Org. Chem.* **1996**, *61*, 3259–3267.
- (3) Wright, A. D.; Wang, H.; Gurrath, M.; Konig, G. M.; Kocak, G.; Neumann, G.; Loria, P.; Foley, M.; Tilley, L. *J. Med. Chem.* **2001**, *44*, 873–885.
- (4) Balde, S. E.; Andolfi, A.; Bruyère, C.; Cimmino, A.; Lamoral-Theys, D.; Vurro, M.; Van Damme, M.; Altomare, C.; Mathieu, V.; Kiss, R.; Evidente, A. *J. Nat. Prod.* **2010**, *73*, 969–971.
- (5) Gao, H.; Zehl, M.; Kaehlig, H.; Schneider, P.; Stuppner, H.; Moreno y Banuls, L.; Kiss, R.; Kopp, B. *J. Nat. Prod.* **2010**, *73*, 603–608.
- (6) Lamoral-Theys, D.; Andolfi, A.; Van Goietsenoven, G.; Cimmino, A.; Le Calvé, B.; Wauthoz, N.; Mégalizzi, V.; Gras, T.; Bruyère, C.; Dubois, J.; Mathieu, V.; Kornienko, A.; Kiss, R.; Evidente, A. *J. Med. Chem.* **2009**, *52*, 6244–6256.
- (7) Van Goietsenoven, G.; Andolfi, A.; Lallemand, B.; Cimmino, A.; Lamoral-Theys, D.; Fras, T.; Abou-Donia, A.; Dubois, J.; Lefranc, F.; Mathieu, V.; Kornienko, A.; Kiss, R.; Evidente, A. *J. Nat. Prod.* **2010**, *73*, 1223–1227.
- (8) Ciavatta, M. L.; Fontana, A.; Puliti, R.; Scognmaglio, G.; Cimino, G. *Tetrahedron* **1999**, *55*, 12629–12636.
- (9) Ciavatta, M. L.; Gavagnin, M.; Manzo, E.; Puliti, R.; Mattia, C. A.; Mazzarella, L.; Cimino, G.; Simpson, J. S.; Garson, M. J. *Tetrahedron* **2005**, *61*, 8049–8053.
- (10) Dumont, P.; Ingrassia, L.; Rouzeau, S.; Ribaucour, F.; Thomas, S.; Roland, I.; Darro, F.; Lefranc, F.; Kiss, R. *Neoplasia* **2007**, *9*, 766–776.
- (11) Mijatovic, T.; Mathieu, V.; Gaussin, J. F.; De Neve, N.; Ribaucour, F.; Van Quaquebeke, E.; Dumont, P.; Darro, F.; Kiss, R. *Neoplasia* **2006**, *8*, 402–412.
- (12) Lefranc, F.; Mijatovic, T.; Kondo, Y.; Sauvage, S.; Roland, I.; Krstic, D.; Vasic, V.; Gailly, P.; Kondo, S.; Blanco, G.; Kiss, R. *Neurosurgery* **2008**, *62*, 211–222.
- (13) Branle, F.; Lefranc, F.; Camby, I.; Jeuken, J.; Geurts-Moespot, A.; Sprenger, S.; Sweep, F.; Kiss, R.; Salmon, I. *Cancer* **2002**, *95*, 641–655.
- (14) Yao, Y.; Jia, X. Y.; Tian, H. Y.; Jiang, Y. X.; Xu, G. J.; Qian, Q. J.; Zhao, F. K. *Biochim. Biophys. Acta* **2009**, *1794*, 1433–1440.
- (15) Ingrassia, L.; Lefranc, F.; Dewelle, J.; Pottier, L.; Mathieu, V.; Spiegl-Kreinecker, S.; Sauvage, S.; El Yazidi, M.; Dehoux, M.; Berger, W.; Van Quaquebeke, E.; Kiss, R. *J. Med. Chem.* **2009**, *52*, 1100–1114.
- (16) Mathieu, V.; Pirker, C.; Martin de Lassalle, E.; Vernier, M.; Mijatovic, T.; DeNeve, N.; Gaussin, J. F.; Dehoux, M.; Lefranc, F.; Berger, W.; Kiss, R. *J. Cell Mol. Med.* **2009**, *9B*, 3960–3972.
- (17) Lefranc, F.; Brotchi, J.; Kiss, R. *J. Clin. Oncol.* **2005**, *23*, 2411–2422.
- (18) Soengas, M. S.; Lowe, S. W. *Oncogene* **2003**, *22*, 3138–3151.
- (19) El Maalouf, G.; Le Tourneau, C.; Batty, G. N.; Faivre, S.; Raymond, E. *Cancer Treat. Rev.* **2009**, *35*, 167–174.
- (20) Denlinger, C. E.; Rundall, B. K.; Jones, D. R. *Semin. Thorac. Cardiovasc. Surg.* **2004**, *16*, 28–39.
- (21) D’Amico, T. A.; Harpole, D. H., Jr. *Chest Surg. Clin. N. Am.* **2000**, *10*, 451–469.
- (22) Savage, P.; Stebbing, J.; Bower, M.; Crook, T. *Nat. Clin. Pract. Oncol.* **2009**, *6*, 43–52.